# Photoelastic and Finite Element Analysis of Embankments Constructed Over Soft Soils

ROBERT L. THOMS and ARA ARMAN, Louisiana State University

The objective of this study was to determine displacements and stresses beneath embankments constructed over soft organic soils (muck) using experimental models and the finite element method. This study was motivated by the fact that embankments are frequently constructed over soft organic soils in southern Louisiana, and the analysis of such embankments is necessary in order to effect a possible savings in construction and maintenance costs. Stresses and displacements were determined experimentally and numerically for model embankments that underwent large deflections when constructed over models of trenched and untrenched soft soils. In the experimental phase of the study, grid and photoelastic methods were used to determine deformations and stresses in the model soil, which consisted of a soft gelatin mix with an embedded ink grid. A gelatin slab, which modeled a cross section of the soil supporting an embankment, was formed in a tank with glass sides. Model embankments were placed in the tank on the gelatin, and resulting grid deformations and photoelastic fringes in the gelatin were photographed.

In the numerical phase of the study, the finite element method was used to determine stresses and displacements in the soil. Experimental and numerical results for maximum normal and shearing stress along the centerline beneath the embankments were compared with results obtained by classical linear elasticity. For embankments undergoing large deformations, where analysis by the classical theory using small deformation restrictions and superposition principles is suspect, it was found that the stress values were bounded above by the classical solution in the case of maximum shear stress and were very close to those predicted by the classical solution in the case of normal stress.

It is concluded that the designer is conservative in using the classic Boussinesq approach in predicting both maximum shear stress and maximum vertical normal stress along the centerline and beneath an embankment undergoing large deformations. Where trenching is used, negative (upward) as well as positive (downward) displacements should be taken into account in estimating the area of the net cross section of an embankment. Trenching is not recommended for the placement of embankments on soft foundations unless (a) the trench is to be used as an economical waterway to transport bulk embankment material and equipment for the construction, or (b) the trenching operation will remove soft material and expose stiffer layers with higher bearing capacity. Untrenched embankment configurations produced no stress concentrations beneath the embankment.

• IN DETERMINING the state of stress beneath an embankment, it has been traditional to apply the linear theory of elasticity. The general assumptions made in the linear

Paper sponsored by Committee on Embankments and Earth Slopes.

theory of elasticity are that (a) the material is continuous, homogeneous, and isotropic; (b) the stress-strain relations are linear and obey Hooke's law; and (c) only small deformations occur.

Some obvious deviations from these assumptions occur in natural soils, especially in muck. Natural soils are not homogeneous; the compressibility of the soil in the foundation varies with depth. However, it was demonstrated that, in clays of moderate or high plasticity, the modulus of elasticity is practically independent of depth (1). Taylor (2) suggested that in many cases the variation of the stress-strain relations with regard to depth is not very large and the overall action is about the same as in the hypothetical case, in which the moduli of elasticity are constant and equal to the average value.

Stress-strain relations for soils are known to be frequently nonlinear. The usual procedure used in the analysis of such soils is to estimate an approximating "effective reaction" modulus.

Finally, the deformation occurring in soils can be quite large, thus violating the third assumption previously listed. In this case the stress state predicted by the linear theory of elasticity is obviously suspect to a degree determined by the magnitude of deformation occurring. Despite these violations of the basic assumptions of linear elasticity, this theory has been applied extensively with apparent good sucess (3).

This report presents the summary of work performed using models and a numerical analysis approach to determine the state of stress existing beneath an embankment placed on a soft soil such as muck. It was assumed throughout this study that finite deformations of the embankment could occur, and that the use of an effective reaction modulus was adequate for representing the material behavior of the soft soil.

## REVIEW OF PAST WORK

### Studies Based on Linear Elasticity

In 1885 Boussinesq derived a detailed and simple solution for determining the state of stress in a semi-infinite elastic isotropic solid subjected to a point load. Boussinesq's derivation has been perhaps the most frequently used solution for determining stress states in soils underlying embankments.

In 1920 Carothers (4) published solutions he developed for the stress distribution produced by triangular, trapezoidal, and terrace loading. Recently semi-empirical equations for evaluating the stresses in a nonhomogeneous foundation were presented by Huang and Zhang (5). Equations for stress in anisotropic soils were developed recently by Barden (6). Jurgenson (7) proposed a method for the analysis of embankment foundations that are homogeneous to an indefinite depth. Gilboy (8) proposed a method for the analysis of embankment foundations using Boussinesq's equations.

Perloff (9) recently analyzed embankments assumed to be continuous with the supporting soil by the complex variable technique of Muskhelishvili for linear elasticity. This work apparently represents the most complete analysis using linear elasticity to date. His analysis assumed the embankment and supporting soil to have the same material properties.

### Experimental Studies Using Gelatin as the Model Soil

In constructing the models to be tested in this study, gelatin was used to simulate soft soil occurring in the natural state. In the area of soil mechanics problems, Farquharson and Hennes (10) were the pioneers with the first significant study using gelatin in conjunction with the method of photoelasticity.

In 1966 Richards and Mark (11) published the results of their work dealing with the use of gelatin for photoelastic studies of gravity structures. Their technique is general and has the capability of treating many interesting problems.

### Review of the Finite Element Method

The numerical analysis phase of this study was based on the finite element method. The literature on applications of the finite element method is extensive, and the reader

is referred to works by Zienkiewicz and Cheung (12) and Przemieniecki (13) for a relatively complete survey through 1966. In the area of soil mechanics, the finite element method was applied by Clough (14), Zienkiewicz (12), Girijavallabham and Reese (15), and others. These studies, as well as Perloff's (9) exact solution by Muskhelishvili's methods, were restricted to the use of small deflection theory.

Finite element methods for the treatment of nonlinear problems involving large deflections have been presented and several laternate approaches are available. The method used in this study is due to Argyris (16) and involves applying increments of load in a sequence in order to keep the problem linear within any one loading increment.

Another source of difficulty is nonlinear material behavior. If time-dependent material behavior is significant, then the problem is complicated further. The determination of a realistic numerical representation of nonlinear time-dependent material behavior is a formidable task. This particular problem was not studied in this project.

## DESCRIPTION OF THE MODEL STUDY

The model study consisted essentially of constructing a model of an embankment over muck. The model embankment was loaded and displacements and stresses were obtained. Then modeling laws obtained from dimensional analysis were used to predict qualitatively and quantitatively the characteristics of displacement and stress distributions. Gelatin was used to simulate muck in the model, and photoelastic and grid methods were used to determine stresses in the gelatin. Displacements were measured by using a grid system embedded in the gelatin.

Figure 1 shows the type of prototype embankments considered, along with a schematic diagram of a model representing the prototype. The model is based on certain idealizations of the prototype that will now be considered.

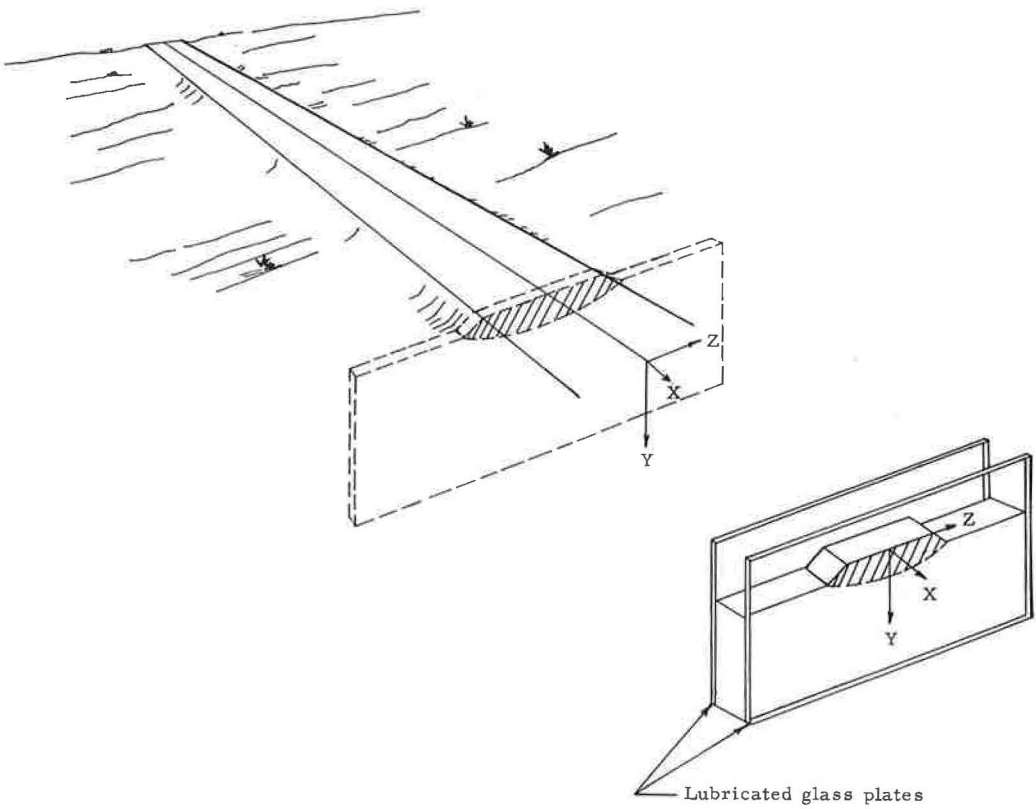


Figure 1. Idealized prototype embankment and model.

## Assumptions Concerning the Actual Embankment

The following simplifying assumptions were made concerning the actual embankment (or prototype):

1. It was assumed that the muck was homogeneous in character and infinite in extent horizontally and semi-infinite vertically.
2. The embankment was assumed to be infinitely long with constant cross sections. Thus, the displacement of a typical cross section of the loaded prototype could be represented by the behavior of a slab of material constrained between two parallel lubricated plane surfaces (state of plane strain). Even in an actual prototype that varies with length, the typical cross sections at several stations could be represented approximately by appropriate models such as shown in Figure 1.
3. It was assumed that values of displacement and stress in the prototype were desired only after an initial significant displacement of the muck had occurred.
4. It was assumed that significant displacement of the muck occurred in a relatively short time after loading and that thereafter the embankment did not settle greatly. Hence, the variations of gelatin properties in the model with respect to time were considered to be a property of the model and were not correlated with variations of such properties with respect to time in an actual embankment. Essentially the prototype was assumed to have effective material properties that were independent of time.

It should be noted that the use of gelatin, which is essentially incompressible and viscoelastic, eliminated the possibility of considering model soil deformations resulting from consolidation and plastic flow.

Based on the foregoing assumptions, the following variables were assumed significant for geometrically similar embankments:

$$u = f(L, W, E, \tau, \mu) \tag{1}$$

The symbols are defined in the Appendix.

The value of Poisson's ratio was assumed to be the same in the model and prototype, i.e., $\mu = 0.5$. Consequently, the following dimensionless products were found by inspection of the remaining variables:

$$\frac{\mu}{L} = f\,\frac{E}{WL}, \frac{\tau}{WL} \tag{2}$$

The characteristic length L used was half the width of the crown c of the embankment. The following modeling laws were written using the dimensionless products given previously:

$$(u)_p = \frac{(c)_p}{(c)_m}\,(u)_m \tag{3a}$$

$$(\tau)_p = \frac{(W\,c)_p}{(W\,c)_m}\,(\tau_m) \tag{3b}$$

$$(E)_p = \frac{(W\,c)_p}{(W\,c)_m}\,(E_m) \tag{3c}$$

## Description of Experimental Apparatus and Technique

Because a semi-infinite slab of soft soil loaded by body forces was being modeled, it was necessary to reduce the edge effects of the model boundary by building a tank that was large relative to the model embankments studied. A large model was also nec-

essary to reduce the difficulty of measuring strains resulting primarily from body-force loading.

The embankment and supporting soil models were formed in a steel-framed tank that was 3 in. wide and had clear glass sides 30 in. deep and 60 in. long (Fig. 2). Each of the glass walls was constructed of a 1-in. thick tempered glass plate on the outside and a ¼-in. stress-free glass plate on the inside. Sandwiched between the two glass plates was a sheet of Polaroid Corporation Circular Polarizing Material No. HNCP-37, 19 in. by 44 in. by 0.02 in. (Fig. 3).

Figure 2. Model casting and testing tank.

The two criteria used in developing a technique for embedding a grid in the model were to obtain a grid system that (a) would have well-defined lines with precise dimensions and (b) would not disrupt the characteristics of the gelatin either by adding strength to it or by reducing its strength.

The technique used was somewhat similar to that used by previous workers using an embedded grid method (17). A frame was fabricated of aluminum channels that would be inside the model tank. Holes were drilled at ½-in. intervals in the channels so that a rectangular gridwork of taut nylon string could be suspended in the gelatin mix. After the mix solidified, ends of the string outside the tank were soaked in ink and the strings withdrawn. Traces of the holes were then left embedded in the gelatin for reference purposes.

Before the grid frame was placed in the tank, the tank was prepared for the gelatin solution. The inside of the tank was washed thoroughly with a mild detergent and warm water. Then a solution of water and zepherine chloride was applied to kill all existing bacteria that could attack the solidified gelatin. The sides of the tank were allowed to dry, and all inside surfaces were coated with Dow-Corning-7 Mold Release Compound to minimize the adhesion of the solidified gelatin to the glass. Following the preparation of the tank and the grid frame in the manner described, the grid frame was lowered into the tank and leveled in order to present a horizontal and vertical grid system.

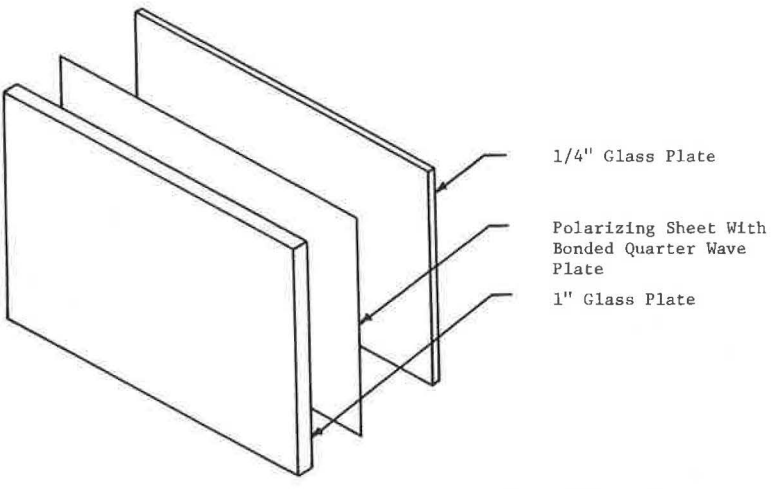


Figure 3. Arrangement of polarizing sheets in modeling tank.

The gelatin mix used to model muck was composed of powdered bone gelatin, glycerine, and sodium propionate (a preservative). The mixtures, weighing approximately 190 lb each, consisted of 5, 5½, or 6 percent gelatin (depending on stiffness desired), 5 percent glycerine, and 1 percent sodium propionate by weight, with the balance being water at 140 F. The solution was allowed to cool to 110 F before it was pumped into the tank.

A smaller tank, 8 in. wide, 10 in. long, and 1.53 in. deep, was manufactured using an aluminum frame and ½-in. thick Plexiglas walls. A ½-in. by ½-in. grid made of braided nylon line was strung across the aluminum channels of the frame through holes drilled in the center of the channels. This tank was designed to be used as a calibration specimen in conjunction with the model tank.

Both the embankment model tanks and calibration specimen tanks were filled with gelatin at the same time, were covered, and were kept in the same environment (an air-conditioned laboratory) until the gelatin had solidified and was ready for loading.

### Construction of the Model Embankments

The model embankments were constructed of two different materials and were placed on two different foundation cross sections. Glass beads of the type used for striping paint were used to simulate cohesionless material, and models of embankments cut from solidified gelatin blocks were used to represent cohesive material.

The embankment models were placed on foundations simulating both on-grade and ditched cross sections. "Ditching" of the model soil was performed by placing in the gelatin a trapezoidal block of lubricated wood having the cross section of the desired ditch. The block was placed before solidification and was removed after solidification of the gelatin. Thus, a clear-cut, well-defined ditch was left in the foundation material.

Where glass beads were used, the loading was performed by pouring beads on the foundation in different manners, representing various loading or construction methods in the field. Model embankments were built in uniform layers or in concentrated loading sequences.

Where cohesive embankments were used, the block of gelatin, shaped as an embankment, was placed on top of the foundation in a single operation. The use of various loading techniques, foundation cross sections, and embankment materials yielded qualitative information concerning the construction sequence, the effect of geometrics, the effect of "ditching" operations, etc. In addition, similar information was obtained by placing berms on each side of the embankments.

## THE CALIBRATION SPECIMEN

In order to relate the measured values of strain and the photographed isochromatic fringes to normal stresses and maximum shear stresses respectively, it was necessary to determine the values of the modulus of elasticity, E, and the model fringe value, $f_\sigma$. This was accomplished by the use of a calibration specimen.

The method of calibration was developed by Frocht (18) and Durelli (17) and later used by Richards and Mark (11). This method consists of placing on end in the polariscope a rectangular block composed of the same material as the model and measuring deformations and the locations of horizontal fringes. The block was cast flat and consequently the deformations and fringes resulting in the block when it was placed on end were due to the weight of the block itself. The specimen was confined between two parallel Plexiglas plates with spacers 1.53 in. deep. Thus, a state of plane strain existed. Silicone lubricants were used between the gelatin and the plates to ensure that friction did not affect the results.

The block deflected under its own weight. The vertical normal stress at any point in the gelatin was then determined by the equation

$$\sigma_y = \rho y \tag{4}$$

where $\rho$ is the specific weight of the gelatin and y is the vertical distance from the top to any point where the stress is desired. A Cartesian x-y reference frame in the mid-

plane of the calibration specimen was assumed. Because $\sigma_x = 0$, i.e., the model was unconfined in the horizontal or x direction, the maximum shear stress was

$$\tau_{max} = \frac{\sigma_y}{2} = \frac{\rho y}{2} \tag{5}$$

Using the embedded grid, the strains $\epsilon_{xx}$ and $\epsilon_{yy}$ could be determined at any point. Because for this case the x and y axes were also the principal axes, the relationship between the maximum shear strain and the strains in the x and y directions was

$$\gamma_{max} = \epsilon_{xx} - \epsilon_{yy} \tag{6}$$

Therefore, the shear modulus was attainable from

$$G = \frac{\tau_{max}}{\gamma_{max}} = \frac{\rho y/2}{\epsilon_{xx} - \epsilon_{yy}} \tag{7}$$

Values of G were determined from data collected at several points within the calibration specimen and then averaged.

Then, the modulus of elasticity was found by the relationship $E = 2(1 + \mu)\,G$. The gelatin was assumed to be essentially incompressible, which implied $\mu = 0.05$. Therefore $E = 3.0\,G$.

The model fringe value was determined from basic equations relating shear stress to fringe order. From photoelasticity theory (18),

$$f_\sigma = \frac{2\tau_{max}h}{n} \tag{8}$$

The maximum shearing stress from Eq. 5 substituted into Eq. 8 yields

$$f_\sigma = \frac{\rho y h}{n} \tag{9}$$

Thus, for several values of y and the corresponding values of n, an average value of the model fringe value was obtained for one specific time and gelatin mixture.

## DETERMINATION OF STRESS AND STRAIN

### Methods of Determining Stress and Strain

The Lagrangian description of the engineering definition of strain was used throughout the study (21). Values of normal strain were obtained by using a 1-in. (undeformed) line segment for a reference length in the embedded grid in the gelatin model. It should be noted that the large size of the model permitted the use of a large reference length.

Because gelatin is incompressible ($\mu = 0.5$), it was not possible to determine explicitly normal stresses directly from normal strain in the plane strain case. For plane strain, assuming that Hooke's laws are valid,

$$\sigma_y = \frac{E(1 - \mu)}{(1 + \mu)(1 - 2\mu)} \left(\epsilon_y + \frac{\mu}{1 - \mu}\,\epsilon_x\right)$$

which becomes meaningless as $\mu \to 0.5$. However, the values of shearing stress (and effective stress) can be obtained by using measurements of the deformed grid and data from the calibration specimen.

The shear difference method (19) was used in conjunction with shear stress determined as noted previously to compute vertical normal stress at any point in the gelatin. The shear difference method is based on approximate integration of the equations of equilibrium, and no additional approximations are introduced for large strain analysis as compared to small strain analysis, provided that the final geometry of the deformed model is used. It should be noted that the shear difference method required an assumption on the "starting" value of the vertical normal stress at the surface of the gelatin. Away from the model embankment the vertical normal stress was obviously zero, but under the embankment it was assumed that the vertical stress was equal to the height of the embankment times the specific weight of the model embankment material. This is the assumption used in the classical solution for stress beneath embankments; however, some investigators have recently questioned this assumption.

Maximum shear stresses were also determined in the gelatin by using photoelasticity theory. The theory is essentially the same as discussed previously in the description of the calibration specimen, and involved photographing and analyzing fringes obtained through the loading of the birefringent gelatin "soil".

It was assumed that at any instant of time the time-dependent gelatin possessed the linear stress-strain relationship $\tau/\gamma = G$. This was justified by plotting a series of stress-strain curves at predetermined times for the calibration specimen. At any one time the curves were found to be linear, thus making it necessary only to photograph the model and to calibrate the specimen simultaneously in order to use the equation given.

## Comparison of Stress Values

Figure 4 shows maximum shear stress values down the centerline beneath the model embankment as determined by the grid method and photoelastic method. The values obtained by each of the two experimental methods were in adequate agreement. Also shown is a plot of the maximum shearing stress as given by the solution of Boussinesq. The largest maximum shearing stress obtained experimentally was approximately 80 percent

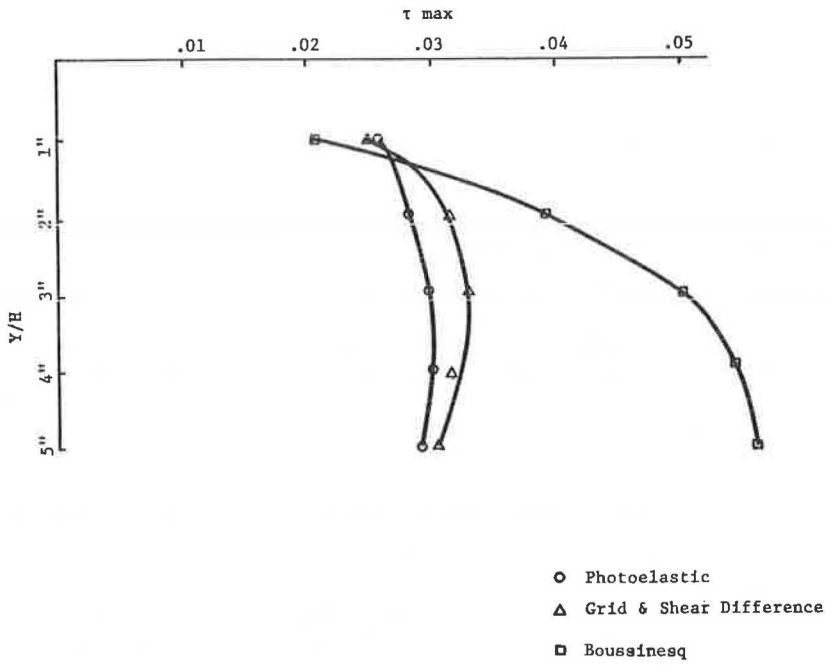


Figure 4. Theoretical and experimental stresses under an embankment.

smaller than the largest shearing stress obtained by the Boussinesq solution. However, while the Boussinesq solution is valid only for relatively small displacements (as would occur for stiff soils), the experimental results were obtained from work with simulated muck where large displacements have occurred.

Plots of superimposed grids before and after deformation for each of the three embankment types were studied. In addition, plots of values of vertical strain, as determined directly from the embedded deformed grid lines in the loaded gelatin model, were made. These plots, in addition to the plots of directions of maximum shearing stress at preselected discrete points and plots of vertical stresses as obtained by the shear difference method in conjunction with values of stress measured from the embedded deformed grid, were analyzed to correlate experimental values with values predicted by the classical linear theory of elasticity.

Thus, experimentally determined values of maximum shearing stress in soft soils beneath the center of the embankments appeared to be appreciably less (80 to 90 percent) than those predicted by the classical linear theory of elasticity that assumes only small displacements occur. On the other hand, maximum vertical normal stresses appeared to decrease less rapidly with depth beneath the model embankment that underwent large displacements.

## Analysis by the Finite Element Method

A study was performed to test the feasibility of using the finite element method to analyze embankments constructed over soft soils where large displacements would occur. The effects of changes in geometry were accounted for by using the geometric stiffness matrix approach of Argyris (16).

The analysis necessary for the finite element method is phrased most conveniently in terms of matrix notation. The set of equations relating loads and displacements at the model points of the body can be written $[K]\{u\} = \{F\}$, where $[K]$ is a square matrix with the number of rows or columns equal to the number of displacement components in the finite element model of the body. Also, $\{u\}$ and $\{F\}$ are column matrices with the same number of rows. The matrix $[K]$ is referred to traditionally as the stiffness matrix, and the $\{u\}$ and $\{F\}$ matrices are referred to respectively as the displacements and force vector. The equation can be regarded as a set of linear algebraic equations involving the unknown displacements $\{u\}$, which can be solved by some appropriate method. With the displacements determined, it is possible to calculate approximate values of stress within any one element.

Because the scope of the numerical analysis of the study was limited to a feasibility study, details on the computer program employed have been omitted. The program employed can be used to account for large deformations and to represent a piecewise linear effective stress-strain relationship for the soil.

To verify the computer program written for this study, the finite element method was used to compute the deflections and stresses in a carefully controlled gelatin calibration specimen. The resulting computed deflection was then compared to the measured deflection of the actual calibration specimen. The material properties of the gelatin specimen were obtained and used in the numerical model of the same specimen. Agreement between the loaded configuration of the physical and numerical calibration specimens was excellent. A finite element analysis that did not take

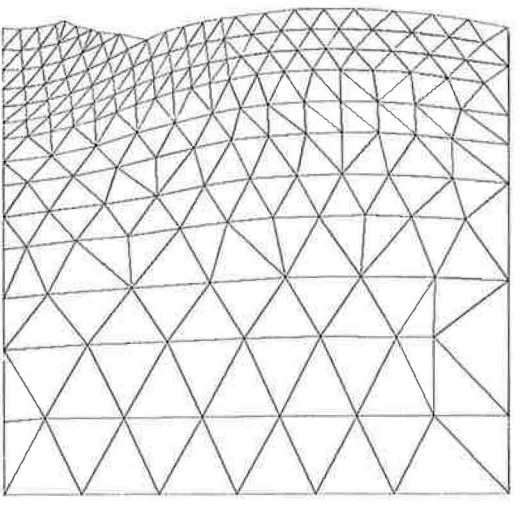

Figure 5. Finite-element model of embankment with total load.

into account large changes in geometry differed in deflections by approximately 15 percent from the plotted specimen shown. This justified considering the effect of large deformations.

The finite element method used in this study to analyze large deflections employed the technique of applying the load in increments. The problem was regarded as linear for each increment of load. The final configuration represented the accumulated effect of the incremental loadings. Figure 5 shows the final deflected configuration of a finite element model of an embankment in which the loading was applied in four increments.

Figure 6 shows plots of maximum shear stresses beneath the embankment down the centerline as computed by Perloff (9) and by the finite element method used in this study. Also shown are plots of maximum shear stress obtained by the experimental method used in the current study and plots of stress obtained by the Boussinesq solution (classical method). It is of interest to compare the various solutions to determine if the classical small deformation theory (Boussinesq, Perloff) yields results close to those predicted by taking large deformations into account.

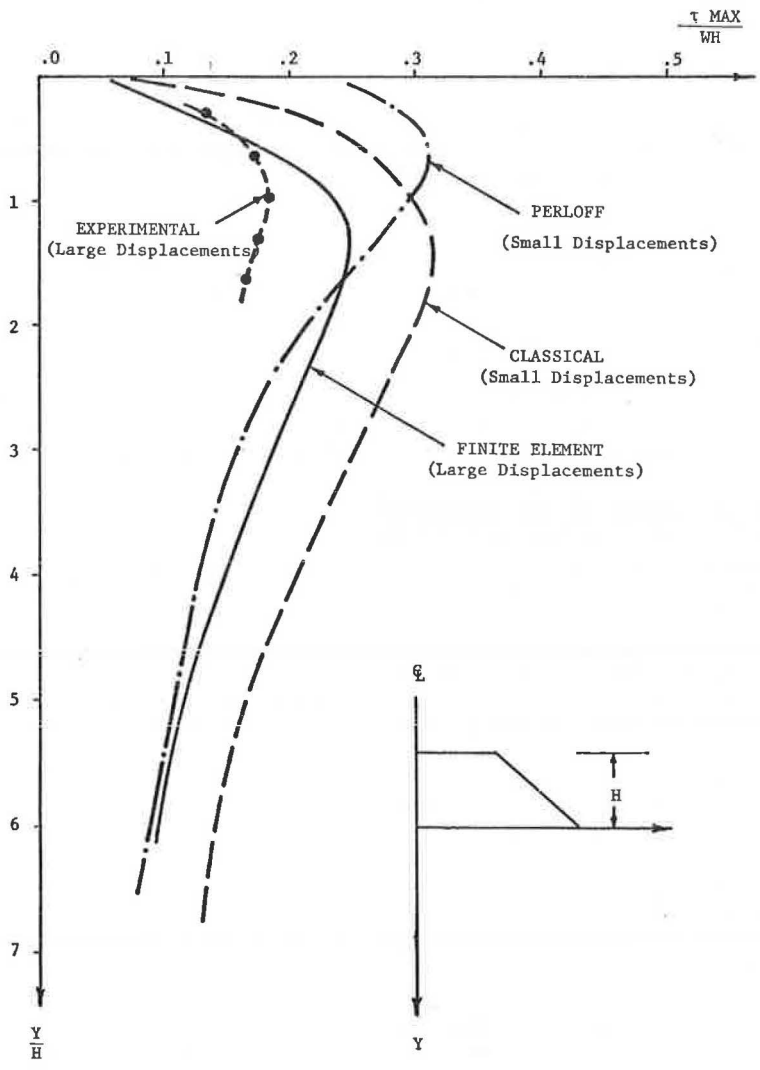


Figure 6. Maximum shear stress beneath embankment.

The finite element approach yields a maximum shearing stress value that is approximately midway between those values determined experimentally and those values determined by small-deformation methods. Using the finite element approach, the maximum stress is predicted to occur at a distance (measured in the undeformed material) beneath the embankment that is approximately equal to that predicted by the classical approach. The experimental method yields results that agree approximately with the finite element method until the experimentally determined maximum stress value is obtained; then the values diverge.

Figure 7 shows a plot of vertical normal stresses beneath the embankment down the centerline. Beneath the embankment the finite element solution is close to the classical assumption, and then it rapidly approaches Perloff's solution (9). The experimental solution for normal stress was "started" at the level of stress as calculated by the

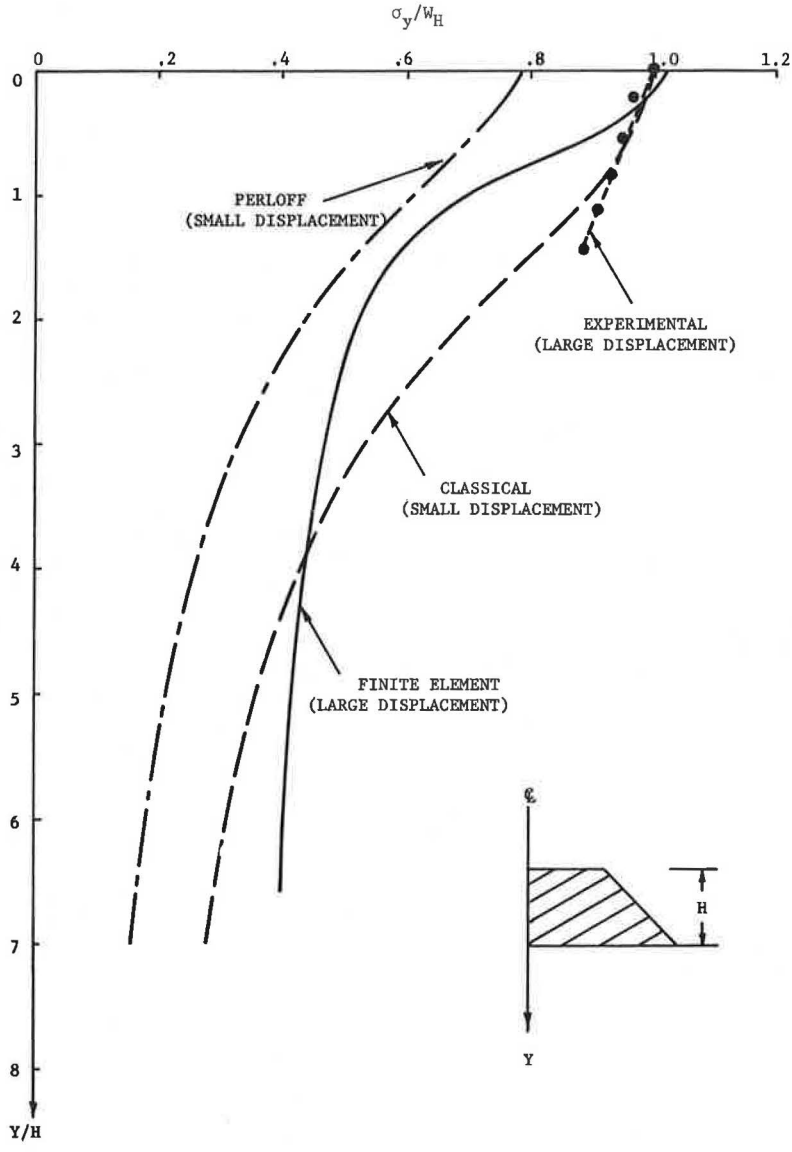


Figure 7. Vertical normal stress beneath embankment.

classical method. The shape of the plotted curve of the experimentally determined values apparently agrees more closely with the curve corresponding to the classical solution.

In summary, it appears that for embankments undergoing large displacements, the maximum shearing stresses beneath the embankment along the centerline are less than those predicted by small deformation theory methods. However, certain precautionary comments should be added. The shearing stress may well increase (from that predicted by small deformation theory methods) at other locations away from the centerline. Finally, the finite element study was preliminary in nature because it was essentially a feasibility study. Additional study of this method for cases where large time-dependent deformations occur is presently in progress.

## QUALITATIVE ANALYSIS OF MODEL FOUNDATIONS

Loading tests performed on trenched and untrenched embankment foundations were analyzed for this study. Embankments with and without berms were loaded on both types of foundations, and the results of each of these tests were analyzed.

### Qualitative Analysis of Trenched Foundations

Trenched model foundations were loaded with embankments both with and without berms as outlined previously. The following observations were made as a result of the analysis of these loading tests:

1. The initial trenching operation produced negative vertical displacements (upward) and accompanying negative stress conditions under the trench. These characteristics did not indicate any impending danger of failure. However, in the measurements of the final cross section of a trench in the field, they may cause some confusion unless this rebounding of the bottom of the trench is taken into account.
2. Continued placement of the embankment material developed photoelastic fringes, qualitatively speaking, with a pattern similar to that of stresses developed in an elastic media composed of homogeneous material stressed by an infinitely long load as defined by Boussinesq.
3. After the loading of the embankment without berms was completed, photoelastic fringes developed in the foreslopes of each trench. These fringes were in circular patterns beginning at the bottom of each side of the trench and extending to the surface of the foundation material. These fringes ended either at the toe of the overlying embankment or in the immediate vicinity of the overlying embankment. These stressed surfaces can develop into the local slip-circle-type failure at the toe of the embankment. This type of failure will cause rotation of a part of both the embankment and the foundation material if stressed beyond the strength of that particular section of the material. Thus, the trenched sections filled with noncohesive materials developed stresses that tended to push the foreslopes of the trench in the direction away from the centerline section of the foundation, which also had a stress concentration that could cause secondary failures.
4. Even under excessive loads applied in an effort to cause failure of the foundation, the modeling media (gelatin) did not display any signs of attaining a plastic state of stress. Thus, in all cases tested in this study, it would be improper to compare the results of these tests with theoretical stress distributions based on the theory of plasticity.
5. Negative vertical displacements (mud waves) occurred starting at the toe of each embankment without berms and extending to the rigid boundaries of the model foundation, which were the side walls of the steel tank. Because gelatin is an incompressible material, additional loads extended the mud waves further toward the rigid boundary and produced higher mud waves. The effect of the boundaries in this case was critical. In actual situations, when an embankment is placed in an area where the vertical displacement of the adjacent areas is critical, the boundary effects resulting from the total or partial confinement of the subgrade should be carefully studied.
6. The placing of berms on trenched sections increased the negative vertical displacement (mud waves) by moving the stressed section closer to the rigid boundaries of

the foundation (sides of the modeling tank). However, the placement of berms decreased by 1.8 percent the strain under the center of the embankment of the model material. From a practical standpoint, this improvement is not worthy of any real consideration.

7. Except in one situation, the addition of berms did not contribute to the general stability of the embankment. The exception is that the slip-circle-type stress concentration, which had developed at the foreslopes of the trenches, closed into a loop after the placement of the berms and went deeper into the foundation material. There was no longer any danger of failure at that point. Thus, the use of berms in trenched sections seems justified only when there is a possibility of developing rotational failure at the lateral extremities of the embankment.

8. Embankments, with or without berms, in trenched sections produced larger shear displacements than those produced in untrenched sections with similar material properties.

9. The negative vertical displacement (mud waves) that developed on trenched sections were 2 to 3 times larger than those that developed on untrenched sections.

10. The sequence of loading of the trenched sections did not affect the pattern of the final stress distribution. However, when the loading was performed in such a manner that one part of the total cross section was built up before the rest of the foundation was loaded, local stress concentrations of high intensity were observed during the loading process. These local stress concentrations could develop into local failures. The best results, both from the standpoint of displacement and uniform stress distribution, were obtained by loading the foundation (building up the embankment) in uniform layers throughout the cross section.

11. Because the use of cohesive material in trenched sections is impractical from the standpoint of obtaining compaction, no attempt was made to model a cohesive embankment in a trenched section.

12. The final stress distribution under a trenched section was somewhat similar to the stress distribution under a rigid plug (Fig. 8).

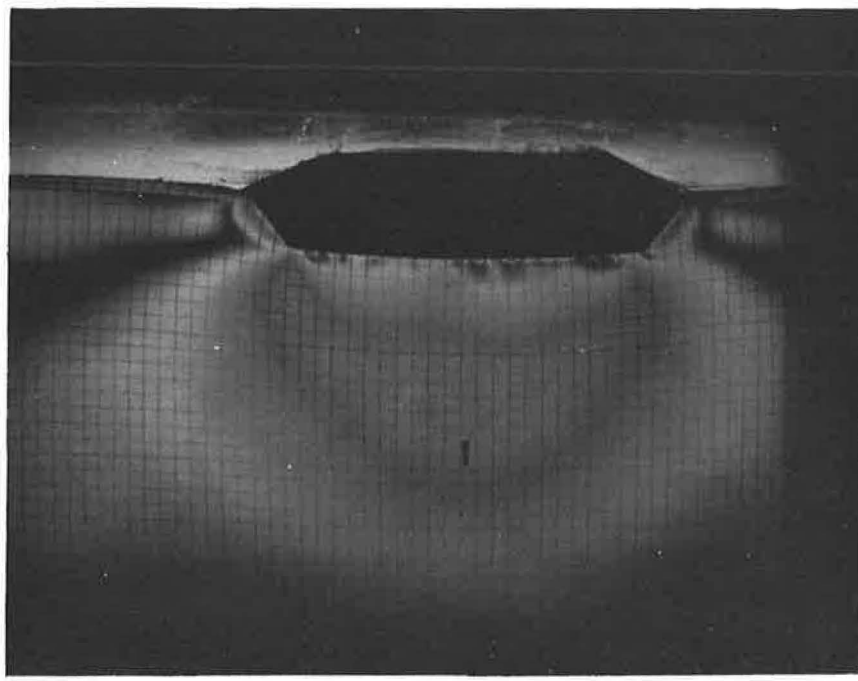

Figure 8. Fringes under trenched section.

Qualitative Analysis of Untrenched Sections

Both cohesive and noncohesive embankments were modeled for untrenched sections. The results of these two types of embankments were similar except as noted in the following. The analysis of untrenched sections after the loading of the embankments of various types (cohesive or noncohesive, with berms or without berms) resulted in the following observations:

1. Untrenched sections produced a stress distribution pattern similar to that of trenched sections except for the lack of circular stress concentrations that had occurred at the foreslopes of trenched sections. Under untrenched sections these stresses were not present.
2. With noncohesive embankments a secondary stress section developed in the foundation adjacent to the toes of the embankment.
3. With cohesive embankments there were no observable secondary stresses in the regions adjacent to the toes of the embankment. Thus, these secondary stress concentrations away from the embankment, which may be critical in cases where other structures exist in these regions, did not form when a cohesive embankment material was used. This indicates that, as a result of the cohesion, the embankment supported itself and did not exert secondary horizontal stresses in a direction away from the centerline of the embankment. Because gelatin was the modeling material for the cohesive embankment, it was possible to observe the stress patterns that developed in the embankment itself. The only stress concentrations that threatened to cause incipient failure were slip-circle-type stress concentrations that developed on the foreslopes of the embankment. Based on these observations, the design of a cohesive embankment on an untrenched section has only two stress criteria to satisfy. These two criteria are (a) that the shear stress should not exceed the shear strength of the material and (b) that slope failures should be prevented.
4. Qualitatively a cohesive embankment on an untrenched section was observed to be the most stable embankment-foundation combination.
5. The addition of berms to embankments on untrenched sections did not contribute to the stability of the embankments. Neither the stress distribution nor the strains or displacements were altered by the addition of berms.
6. When failure was induced by overloading the embankment, initial failure occurred in the vicinity of the toe of the embankment. Here, starting at the surface, the foundation material was put into tension as a result of the excessive displacement that took place under the embankment. This caused tension cracks to open in the regions at the toe of the embankment. After this the material under the embankment started developing fissures and eventually failed. The embankment rotated and in a single mass sank through the fissure that had developed beneath it.
7. Under embankments of approximately the same weight, untrenched sections developed less shear displacement beneath the centerline of the embankment than trenched sections.
8. The mud waves that developed on untrenched sections were considerably less pronounced than those that developed on trenched sections.
9. Untrenched sections did not present any disadvantages when compared to trenched sections. In fact, in only two situations is trenching recommended. Trenching is advisable when the trenches will create a temporary waterway for the transportation of the embankment material. In areas where soft deposits are located, this might be the only way to transport the embankment material. Second, trenching is recommended when the majority of the soft deposits can be removed by the trenching operations. Otherwise, untrenched sections have the advantage of adding a load to the present overburden that, as a result of consolidation, will accelerate the settlement of the embankment and increase the shearing strength of the foundation material.

## CONCLUSIONS

Based on the results of this study, the following conclusions were reached by the researchers:

1. The finite element analysis is a very promising tool for the analysis of distribution of stresses and strains beneath embankments with large shear displacements.
2. Along the centerline beneath embankments undergoing large displacements maximum shear stress is apparently smaller than that calculated by approaches assuming small deformation.
3. Maximum normal stress beneath embankments is apparently no greater than that obtained by approaches assuming small deformation theory.
4. The designer is conservative in using the classical approach (Boussinesq) in predicting both maximum shear stress and maximum vertical normal stress along the centerline and beneath an embankment undergoing large deformations.
5. The use of models for photoelastic analysis, as described in this report, is an effective tool for the qualitative analysis of the overall stress and strain patterns in soils supporting embankments and other adjacent structures.
6. The embedded grid method developed for gelatin models in this study is an effective tool for evaluating large strains and displacements.
7. Where trenching is used, negative (upward) as well as positive (downward) displacements should be taken into account in estimating the area of the net cross section of an embankment.
8. Trenching is not recommended for the placement of embankments on soft foundations unless (a) the trench is to be used as an economical waterway to transport bulk embankment material and equipment for the construction, or (b) the trenching operation will remove soft material and expose stiffer layers with higher bearing capacity.
9. Placement of berms produced no desirable effects in an elastic material except for reducing the stress concentration at the toe of trenched embankments. In a plastic material, however, stability may be enhanced through the use of berms.
10. Untrenched embankment configurations produced no stress concentration beneath the embankment.

## ACKNOWLEDGMENT

The authors would like to extend their thanks to all students, technicians, and clerical and editorial helpers who worked on this study. Special thanks and acknowledgments are due to James O. DeViller, former graduate research assistant, and John Horn, former laboratory assistant, for their work on the experimental phase of this study; to Hector Rosenfeld, former graduate research assistant, and Ronald S. Reagan for their work on the numerical phase of this study; and to Charles Hill and Ann Lewis for their assistance in the photographic and editorial work.

## REFERENCES

1. Finn, W. D. Stress in Soil Masses Under Various Boundary Conditions. Univ. of Michigan, Ann Arbor, unpublished PhD thesis, 1962, p. 10.
2. Taylor, D. Fundamentals of Soil Mechanics. Wiley and Sons, New York, 1960.
3. Turnbull, W. J., Maxwell, A., and Ahlvin, R. G. Stress and Deflections in Homogeneous Soil Masses. Proc. Fifth Internat. Conf. Soil Mechanics, Pt. 2, Paris, 1961, pp. 337-346.
4. Carothers, S. D. Direct Determination of Stresses. Proc. Royal Society of London, Series A, Vol. 97, 1920, pp. 110-123.
5. Huang, Wen-xi, and Zhang, Wen-Zhang. Settlement Analysis of Soil Foundations, of Hydraulic Structure and Stress Distribution in Foundations. Scientia Sinica, Vol. 8, 1959, pp. 1393-1417.
6. Barden, Laing. Stress and Displacements in Cross-Anisotropic Soil. Geotechnique, Vol. 13, 1963, pp. 198-210.
7. Jurgenson, Leo. On the Stability of Foundations of Embankments. Internat. Conf. Soil Mechanics and Foundation Engineering, 1936, pp. 194-200.
8. Gilboy, Glenn. Stability of Embankment Foundations. Trans. Second Conf. Large Dams, Vol. 4, 1936.
9. Perloff, W. H., Baladi, G. Y., and Harr, M. E. Stress Distributions Within and Under Long Elastic Embankments. Highway Research Record 181, 1967, pp. 12-41.

10. Farquharson, F. G., and Hennes, R. G. Gelatin Models for Photoelastic Analysis of Stress in Earth Masses. Civil Engineering, Vol. 10, Pt. 4, 1940, pp. 211-214
11. Richards, R., Jr., and Mark, B. Gelatin Models for Photoelastic Analysis of Gravity Structures. Experimental Mechanics, Jan. 1966, pp. 30-38.
12. Zienkiewicz, O. C., and Cheung, Y. K. The Finite Element Method in Structural and Continuum Mechanics. McGraw-Hill, New York, 1967.
13. Przemieniecki, J. S. Theory of Matrix Structural Analysis. McGraw-Hill, New York, 1968.
14. Clough, R. H. The Finite Element in Plane Stress Analysis. Proc. Second ASCE Conf. on Electronic Computation, Philadelphia, Sept. 1960.
15. Girijavallabham, C. V., and Reese, L. C. Finite Element Method for Problems in Soil Mechanics. Jour. Soil Mech. and Found. Div., ASCE, Vol. 94, No. SM2, March 1968.
16. Argyris, J. H. Matrix Displacement Analysis of Three-Dimensional Elastic Media, Small and Large Displacements. AIAA Jour., Vol. 3, No. 1, Jan. 1965.
17. Durelli, A. J., Phillips, E. A., and Tsao, C. H. Introduction to the Theoretical and Experimental Analysis of Stress and Strains. McGraw-Hill, New York, 1965
18. Frocht, M. M. Photoelasticity, 2 volumes. Wiley and Sons, New York, 1941 and 1948.
19. Dally, J. W., and Riley, W. F. Experimental Stress Analysis. McGraw-Hill, New York, 1965.
20. Arman, A. A New Concept in Design and Construction of Embankments Founded on Muck. Div. of Engineering Research, Louisiana State Univ., 1965.
21. Parks, V. J., and Durelli, A. J. On the Definitions of Strain and Their Use in Large Strain Analysis. Experimental Mechanics, Vol. 7, No. 6, June 1967.

# *Appendix*

## NOTATION

The following symbols are used in this paper:

$L$ = length of embankment;
$u$ = displacement;
$W$ = specific weight of backfill material;
$E$ = modulus of elasticity;
$\tau$ = shearing stress;
$\mu$ = Poisson's ratio;
$K_{()}$ = ratio of model property to prototype property (property in parentheses);
$c$ = width of embankment crown;
$()_p$ = property in parentheses is characteristic of prototype;
$()_m$ = property in parentheses is characteristic of model;
$f_\sigma$ = model fringe value;
$x, y, z$ = rectangular coordinates;
$\sigma$ = normal or principal stress;
$\rho$ = specific weight of the gelatin;
$\epsilon$ = strain;
$G$ = shear modulus;
$h$ = thickness;
$n$ = fringe order;
$l_i$ = initial length of line segment;
$l_f$ = final length of deformed line segment;
$P$ = grid point in gelatin; and
$\gamma$ = shearing strain.